KINETICS PARAMETERS OF THE THERMAL DEHYDROXYLATION OF GIBBSITE AL(OH)3 BY DIFFERENTIAL THERMAL ANALYSIS (DTA)

Djaida REDAOUI[1], Foudil SAHNOUNE[1,2]

(1) Physics and Chemistry of Materials Lab, Department of Physics, University Mohamed Boudiaf of M'sila, 28000, M'sila, Algeria
(2) Research Unit on Emerging Materials (RUEM), University of Setif1, Setif 19000, Algeria

E-mail: djaidaredaoui@gmail.com

Abstract

In this present study, the thermal decomposition of gibbsite $Al(OH)_3$ was studied by the Differential Thermal Analysis (DTA) technique under non-isothermal conditions, the gibbsite powder were carried out between room temperature to 900 °C using heating rates of 5, 10, 15 and 20 °C/min.The obtained DTA curves show two different peaks: the first peak is due to partial dehydroxylation of gibbsite and formation of boehmite, the value of the activation energy (E_A) corresponds to 143 KJ/mol. The second peak corresponds to transformation of gibbsite to χ-Al_2O_3 phase, the activation energy (E_A) was found around to 185 KJ/mol. The values of apparent activation were determined by Ozawa–Flynn–Wall (OFW), Boswell and Kissinger–Akahira–Sunose (KAS) methods and by applying the basic solid-state kinetic equations. The phases formed and the structural changes were investigated by differential thermogravimetry (DTG) and X-ray diffraction (XRD) for gibbsite powder treated at different temperatures from room temperature to 1100 °C.

Keywords: Activation energy, Decomposition kinetics, Differential Thermal Analysis (DTA), Gibbsite.

1- INTRODUCTION

The thermal decomposition of gibbsite to boehmite has been studied by a many authors using a large variety of methods, such as thermal analysis, X-ray diffraction, dilatometry and other methods. Gibbsite or as it called aluminiumtrihydrate ($Al_2O_3.3H_2O$) is the usual precipitation produced from alumina refineries with each sintering process or Bayer [1]. It's have been widely used in many industry applications due to their fine particle size, high surface area and catalytically active surfaces as absorbents, catalysts, catalyst supports, coatings and soft abrasives [2].

According to its stability and other beneficial characteristics is also used to manufacture ceramic materials for refractory, microelectronics and structural applications [3].

In the present work we tried to describe the mechanism and thekinetic parameters of the thermal decomposition of gibbsite such as the activation energy (E_A) and pre-exponential factor (K_0), under non-isothermal conditions and by using two methods different, the first one byutilizeOzawa–Flynn–Wall (OFW), Boswell and Kissinger–Akahira–Sunose (KAS) methods, the second method by applying the basic solid state kinetic equations [4-12].

It is well-known that the thermal decomposition of gibbsite under usually pressures, gives two primary products boehmite and χ-Al_2O_3 phase. In vacuum leads to Al_2O_3 the thermal decomposition being almost amorphous [13].

At a temperature range from 500 to 750 K, it is habitually concluded that the process can be divided into two peaks or two stages: the first one is due to the partial dehydroxylation of gibbsite and formation of boehmite called as reaction (A), the second peak correspond to the transformation of gibbsite to phase χ-Al_2O_3 named as reaction (B).

The 32 solid-state mechanisms are applied for analyzing the DTA data obtained in each stage e.g. the appendix of this paper. The aim of this work is to find the most suitable mechanism and to determine the kinetics parameters of each peak.

2- MATERIALS AND METHODS

The gibbsite used under this investigation was commercially powder called as Aluminum hydroxide $Al(OH)_3$. Its typical analysis is 65% Al_2O_3, 0.15% Na, 0.005% Fe and 0.002% SO_4. The Differential thermal analysis (DTA) and Thermogravimetric analysis (TG) experiments were carried out on gibbsite powder at a temperature range between room temperature and 900 °C at different heating rates 5, 10, 15

and 20 °C/min using a SetaramLABevo TG-DSC 1600 °C equipment, operating under Argon atmosphere. In order to determining the present phases at different temperature we use diffractmeter system XPERT-PRO with scan step size 0.0167.

3- RESULTS AND DISCUSSION

The typical DTA/TG curves of gibbsite powder is showing in Figure 1, the powder was heated from room temperature to 900 °C or in kelvin equal to 1173 K at a heating rate of 10 °C/min. The DTA curve shows clearly that there are three endothermic peaks. The first endothermic peak at 510 K due to the partial dehydroxylation of gibbsite and formation of boehmite (AlOOH), second endothermic peak at 576 K corresponds to transformation of gibbsite to χ-Al_2O_3 phase, another endothermic peak at 793 K due to the decomposition of boehmite and a formation of new phase of alumina as called γ-Al_2O_3[14]. The typical thermogravimetric TG curve reveals the most important weight loss, three steps mass loses are detected. The first mass loss (about 5%) corresponds to partial transformation of gibbsite to boehmite. The next mass loss (about 25%) due to the evaporation of adsorbed water and decomposition of gibbsite to χ- Al_2O_3, one more step of mass loss (about 3%) represent the formation of γ-Al_2O_3.

3.1- X-ray diffraction patterns analysis

In order to determine the chemical composition of gibbsite of course after the required heat treatment the powder were analyzed by X-ray diffraction technique. At room temperature we find that the powder of gibbsite showed essentially reflections of pure gibbsite. The eight powders were heated at different temperature for 2 hours. As seen in Figure 2 from 250 to 450 °C, gibbsite was transformed completely to boehmite. After that from 500 to 900 °C, XRD spectra show clearly that boehmite transformed to amorphous phase of alumina as called to χ- Al_2O_3, When the other powder were heated from 900 to 1100 °C new phase of alumina is apparent named as γ-Al_2O_3. The results are shown in figure. 2.

A widely non isothermal method used to determinate the activation energy (E_A) of gibbsite for each transformation such are Ozawa, Boswell and Kissinger as following eq. (1), eq. (2) and eq. (3) respectively:

$$Ln[\varphi] = -1{,}0518\ \frac{E_A}{RT_P} + C \qquad (1)$$

$$Ln\left[\frac{\varphi}{T_P}\right] = -\frac{E_A}{RT_P} + C \qquad (2)$$

$$Ln\left[\frac{\varphi}{T_P^2}\right] = Ln\left[\frac{RA}{E_A}\right] - \frac{E_A}{RT_P} \qquad (3)$$

Where C is a constant, φ is the heating rate in the DTA; (E_A) is the crystallization activation energy and T_P is the absolute temperature in DTA curves

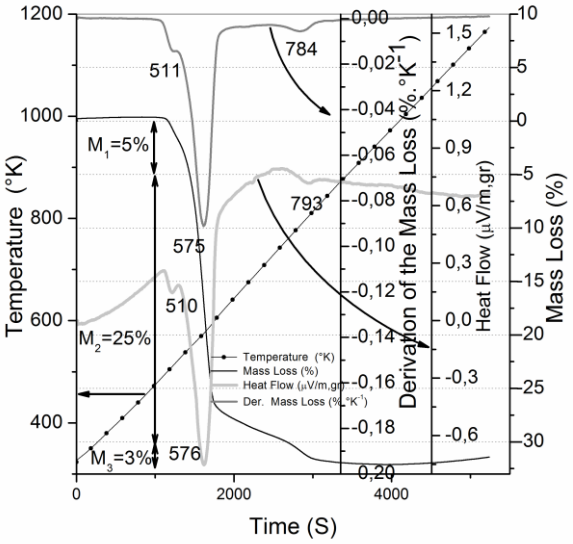

Fig. 1: DTA and TG curves of gibbsite powder heated at 10 °C/min.

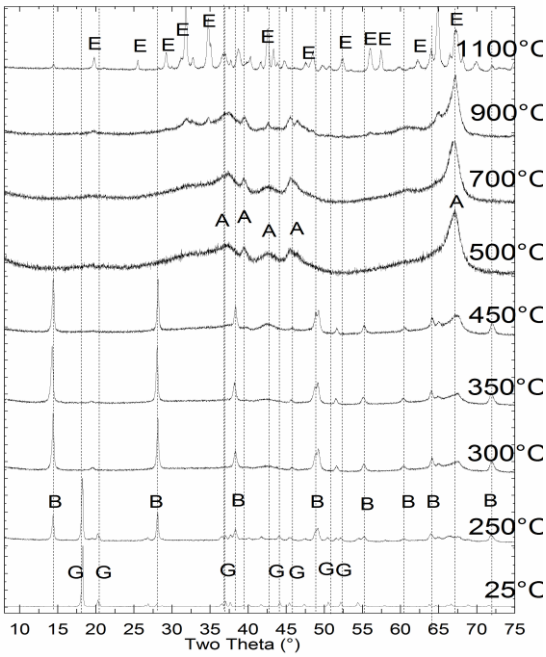

Fig. 2: X-ray patterns of gibbsite powder treated at different temperatures for 2 h, (G) Gibbsite, (B) Boehomite, (A) χ- Al_2O_3 and (E) γ-Al_2O_3.

The results are shown in Figure 3. A plot of ln φ vs. $\frac{1}{T_P}$ and the plot of $\frac{\varphi}{T_P^2}$ versus $\frac{1}{T_P}$ both of them expected to be linear. So the activation energy, E_A, can be attained via this expression.

The values of E_A, r and R^2 (coefficient of determination) determined from slopes of these straight lines are given in tab. 1 at 510 K Reaction (A) due to the partial dehydroxylation of gibbsite and formation of boehmite (AlOOH), the activation energy (E_A) variable from 143 to 147 KJ/mol. Another reaction (B) at 575 K is corresponding to transformation of gibbsite to χ-Al_2O_3phase,the energy of activation in range of 185–190 KJ/mol.

3.2- Determination of mechanism

By applying the basic solid-state kinetic equations we found that the mechanisms function of gibbsite as shown in tab. 2 are depended on the values of g(x) the most likely reaction mechanism was evaluated from the thermal analysis data. Ln [g(x)/T^2] Functions for each mechanism were calculated for each degree of conversions and dependence of this function on 1/T [11].

3-2-1. Kinetic analysis in the temperature range 500–540K

The most mechanism obtained for decom-posetion of gibbsite in the temperature range 500–540K is Avrami-Erofeev eq. (Order=2/3) which called $A_{3/2}$. At heating rates of 5, 10, 15 and 20 °C/min the activation energy (E_A) and the pre-exponential factor (K_0) are 155 to 213 KJ/mol and 3,61.$10^{15}$to 6,87.10^{21} s^{-1} respectively tab. 3.

Figure 4 shows the plot of ln [g(x)/T^2] versus 1/T at each heating rates. The result will be a linear curve with a slope equal to the activation energy (E_A). Also the values of the pre-exponential factor (K_0) are calculated from the intercept values of the plot [12].

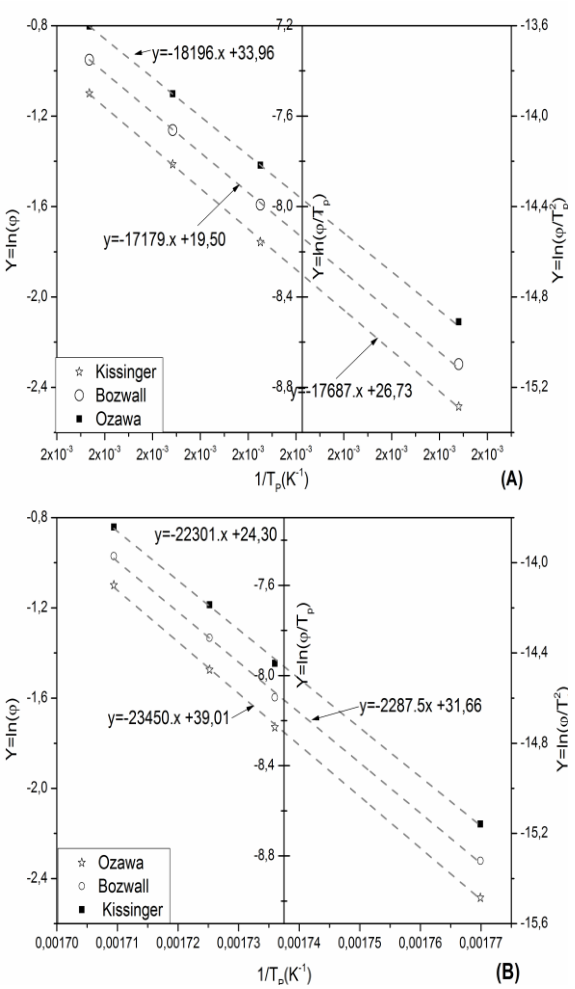

Fig. 3: Plot of y=ln[φ], ln[φ/T_P] and ln[φ/T_P^2] for (A) and (B) reactions

Table 1: the values of E_A, R and R^2 for each reaction

-------	Reaction (A)			Reaction (B)		
Method	**E_A (KJ/mol)**	**R**	**R^2**	**E_A (KJ/mol)**	**R**	**R^2**
Ozawa	143.83	-0.99596	0.98790	185.36	-0.99090	0.97281
Boswell	147.06	-0.99573	0.98722	190.19	-0.99044	0.97146
Kissinger	142.83	-0.99548	0.98648	185.41	-0.98995	0.97000

Table 2: Kinetic parameters of the thermal decomposition of gibbsite

Mech.	g(x)	Reactionprocess	E_A(KJ/mol)	K_0 (1/s)	R	R^2
$A_{3/2}$	g(x)=[-ln(1-x)]$^{2/3}$	Avrami-Erofeeveq. Order =2/3	175.90	6.87.10^{21}	-0.9998	0.99694
F_2	g(x)=(1-x)$^{-1}$-1	second-order	228.33	2.58.10^{23}	-0.9990	0.99819

Table 3: Kinetic parameters and R^2 values determined for $A_{3/2}$ mechanism under non-isothermal condition within conversion range 0.25 ≤x≤0.75

Θ(°C/min)	**E_A(KJ/mol)**	**K_0(1/s)**	**R^2**
5	213.21	$6.87.10^{21}$	0.99656
10	168.70	$9.19.10^{16}$	0.99842
15	155.37	$3.61.10^{15}$	0.99689
20	166.35	$4.75.10^{16}$	0.99590

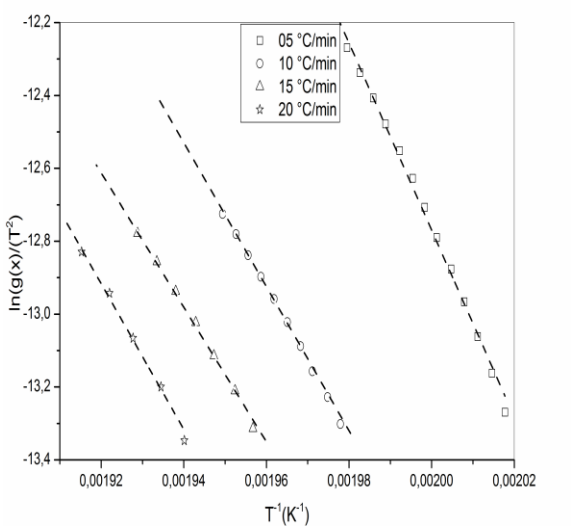

Fig. 4: shows the plot of ln [g(x)/T^2] versus 1/T at each heating rates

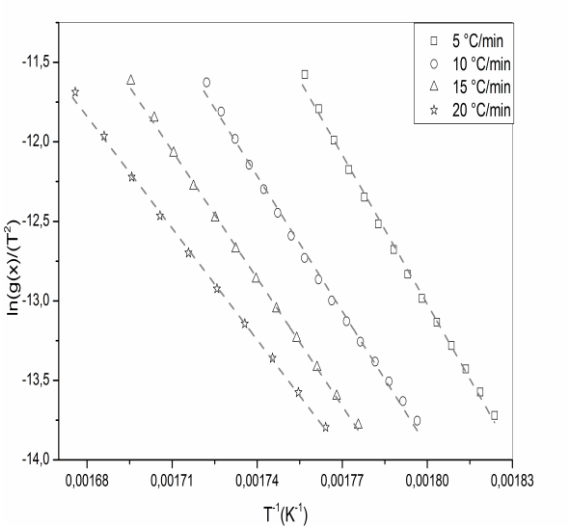

Fig. 5: shows the plot of ln [g(x)/T^2] versus 1/T at each heating rates

3-2-2.Kinetic analysis in the temperature range 540–750 K

The most mechanism in the temperature range 540–750 K is second-order F_2. At heating rates of 5, 10, 15 and 20 °C/min the activation energy (E_A) and the pre-exponential factor (K_0)equal to 195to 260 KJ/mol and $4.07.10^{17}$to $1.03.10^{24}$ s^{-1} respectively in tab. 4.

Figure 5 shows the plot of ln [g(x)/T^2] vs. 1/T at each heating rates. The result will be a linear curve with a slope equal to the activation energy (E_A). Also the values of the pre-exponential factor (K_0) are calculated from the values of the intercept of the plot [11].

Table 4: Kinetic parameters determined for F_2 under within conversion range 0.25 ≤ x ≤0.75

Θ(C°/min)	**E_A(KJ/mol)**	**K_0(1/s)**	**R^2**
5	260.29	$1.03.10^{24}$	0.9974
10	235.87	$3.86.10^{21}$	0.9968
15	222.50	$1.75.10^{20}$	0.9995
20	194.66	$4.07.10^{17}$	0.9988

4. CONCLUSION

Thermal analysis techniques are used in the evaluation of kinetic parameters of solid-state reactions in the dehydroxylation process of gibbsite powder, Among the 32 types of non-isothermal kinetics differential equations just a single mechanism was describe each stage:

The first stage at 510 K which is due to the partial dehydroxylation of gibbsite and formation of boehmite (AlOOH) , the most suitable mechanism is Avrami-Erofeev, eq. Order=2/3:

$$A_{3/2}: g(x) = [-\ln(1-x)]^{2/3}$$

The second stage at 576 K corresponds to transformation of gibbsite to χ-Al_2O_3phase; we find that the most suitable mechanism is controlled by the rate of second-order reaction:

$$F_2: g(x) = (1-x)^{-1}-1$$

Appendix

Determination of example mechanism calculated from Differential Thermal Analysis (DTA) data of each heating rate ($A_{3/2}$). The table listed the values of R^2 obtained over interval $0.25 \leq x \leq 0.75$. The results in bold are marked for the most probable mechanism [14]

Definition of the kinetic function			**Heating rate**			
Sign	**Functionname**	**Formula of g(x)**	**05**	**10**	**15**	**20**
$F_{1/3}$	One-thirdorder	$1-(1-x)^{2/3}$	0,98792	0.99666	0.99457	0.98434
$F_{3/4}$	Three-quartersorder	$1-(1-x)^{1/4}$	0.99412	0.99491	0.99522	0.98219
$F_{3/2}$	One and a half order	$(1-x)^{-1/2}-1$	0.99833	0.99426	0.99082	0.98833
F_2	Second order	$(1-x)^{-1}-1$	0.95681	0.99403	0.99396	0.98281
F_3	Thirdorder	$(1-x)^{-2}-1$	0.99657	0.99646	0.98701	0.98815
$P_{3/2}$	Mampel power law	$x^{3/2}$	0.98142	0.99557	0.99314	0.99876
$P_{1/2}$	Mampel power law	$x^{1/2}$	0.97946	0.99549	0.99221	0.98191
$P_{1/3}$	Maple power law	$x^{1/3}$	0.97778	0.99493	0.99138	0.98999
$P_{1/4}$	Maple power law	$x^{1/4}$	0.97589	0.97445	0.99042	0.98896
F_1	Avrami-Erofeeveq.	$-\ln(1-x)$	0.99665	0.99389	0.99701	0.98404
$A_{3/2}$	Avrami-Erofeeveq.	$[-\ln(1-x)]^{2/3}$	**0.99656**	**0.99656**	**0.99689**	**0.9959**
A_2	Avrami-Erofeeveq.	$[-\ln(1-x)]^{1/2}$	0.99646	0.99646	0.99677	0.98505
A_3	Avrami-Erofeeveq.	$[-\ln(1-x)]^{1/3}$	0.99626	0.99626	0.99651	0.98551
A_4	Avrami-Erofeeveq.	$[-\ln(1-x)]^{1/4}$	0.99604	0.99604	0.99611	0.98543
R_1	Power law	x	0.98096	0.98096	0.99292	0.98507
R_2	Power law	$1-(1-x)^{1/2}$	0.99072	0.99072	0.99528	0.98165
R_3	Power law	$1-(1-x)^{1/3}$	0.99309	0.99309	0.99592	0.98419
D_1	Paraboliclaw	x^2	0.98165	0.98165	0.99324	0.98488
D_3	Jandereq.	$[1-(1-x)^{1/3}]^2$	0.99329	0.99578	0.99408	0.98202
D_4	Ginstling–Brounstein	$1-(2x/3)-(1-x)^{2/3}$	0.98996	0.99712	0.99523	0.98507
D_5	Zhuravleveq.	$[(1-x)^{-1/3}-1]^2$	0.99682	0.99508	0.99493	0.98415
D_6	Anti-Jandereq.	$[(1+x)^{1/3}-1]^2$	0.97763	0.99445	0.99189	0.98705
D_7	Anti-Ginstling–Brounstein	$1+(2x/3)-(1+x)^{2/3}$	0.97902	0.99483	0.99236	0.98106
D_a	Anti-Zhuravleveq.	$[(1+x)^{-1/3}-1]^2$	0.97278	0.99311	0.99029	0.98882
G_1	Otherkineticfunction	$1-(1-x)^2$	0.94857	0.98949	0.98585	0.98415
G_2	uncertainmechanism	$1-(1-x)^3$	0.89924	0.98	0.97483	0.97254
G_3		$1-(1-x)^4$	0.8347	0.9659	0.95873	0.95577
G_4		$[-\ln(1-x)]^2$	0.99674	0.99853	0.98715	0.97558
G_5		$[-\ln(1-x)]^3$	0.99676	0.99854	0.98717	0.98567
G_6		$[-\ln(1-x)]^4$	0.99578	0.99455	0.99372	0.98624
G_7		$[1-(1-x)1/2]^{1/2}$	0.99393	0.99433	0.99272	0.98747
G_8		$[1-(1-x)1/3]^{1/2}$	0.99751	0.99756	0,9825	0.88455

REFERENCES

[1] Z. Wang, L. Yang, J. Zhang, Z.C. Guo, Y. Zhang, Adjustment on gibbsite and boehmite co-precipitation from supersaturated sodium aluminate solutions, T Nonferr Metal Soc, 20, 3 (20l0) 521-527

[2] R. S. Zhou, R. L. Snyder, Structures and transformation mechanisms of the η, γ and θ transition aluminas, ActaCrystallogr B, 47 (1991) 617-630

[3] A.Malki, Z. Mekhalif, S. Detriche, G. Fonder, A. Boumaza, , A. Djelloul, Calcination products of gibbsite studied by X-ray diffraction, XPS and solid-state NMR, J Solid State Chem, 215 (2014) 8-15

[4] F. Benali, M.Hamidouche, H.Belhouchet, cinetique de deshydratation d'un coulis refractaire, Verres, Céramiques & Composites, 5, 1 (2016) 1-6

[5] A. W. Coats, J. P. Redfern, Kinetic parameters from thermogravimetric data, Nature, 201 (1964) 68-69

[6] E. S. Freeman, B. Carroll, The application of thermoanalytical techniques to reaction kinetics, J PhysChem-US, 62 (1958) 394-397

[7] V. M. Gorbachev, A solution of the exponential integral in the non-isothermal kinetics for linear heating, J Therm Anal Calorim, 8 (1975) 349-350

[8] H. H. Horowitz,G. Metzger, A new analysis of thermogravimetric traces, Anal Chem, 35 (1963) 1464–1468

[9] V. Satava, F. Skvara, Mechanism and kinetics of the decomposition of solids by a thermogravimetric method, J Am Ceram Soc, 52(18), (1969)591-595

[10] J. Zsako, Kinetic Analysis of Thermog-ravimetric Data, VI, Some Problems of Deriving Kinetic Parameters from TG Curves, J Therm Anal Calorim, 5 (1973) 239-251

[11] N. Saikia, , P. Sengupta, P. K. Gogoib, P. C. Borthakur, Kinetics of dehydroxylation of kaolin in presence of oil field effluent treatment plant sludge,Appl Clay Sci, 22 (2002)93-102

[12] E. Apaydin-varol,S. Polat, A. E. Putun, Pyrolysis kinetics and thermal decomposition behavior of polycarbonate – a TGA-FTIR study, Thermal Science, 18(3), (2014) 833-842

[13] G. Pokol, , G. Várhegyi, L. Várady, Studies on the kinetics of the gibbsite → χ-alumina reaction, ThermochimActa, 76 (1984) 237-247

[14] P. Ptáček, D. Kubátová, J. Havlica, J. Brandštetr, F. Šoukal, T.Opravil, The non-isothermal kinetic analysis of the thermal decomposition of kaolinite by thermogravi-metric analysis, Powder Technol, 204 (2010) 222-227